UNIVERSITY OF THE WITWATERSRAND

School of Electrical and Information Engineering

21 AUGUST 2020

MACHINE LEARNING DESIGN OF A ROBUST CODEC FOR FADING CHANNEL

Author:
SBONELO MDLULI (1101772)

Supervisor:
PROF. FAMBIRAI TAKAWIRA

Abstract

This paper presents the design and analysis of an adaptive modulation and coding scheme. The scheme is intended for a codec used in a WiFi router. Three modulation and coding schemes are used to develop the codec namely 8QAM and 16QAM with a $1/3$ BCH encoder and 4QAM without error correction. MIMO is used to increase the spectral efficiency of the codec within the fading channel. To make channel prediction possible a linear discrete channel model is presented based on ARMA processes. The presented scheme is operational at a BER threshold of 10^{-3}, with a channel correlation of 0.96 and a noise variance of 3 dB. The adaption parameter defined in this report gives a measure of the effect of the channel and equalizer to SNR. The adaption parameter and the channel model provide the basis of the machine learning model. A neural network and LSTM are used as prediction models for the adapter. The neural network has better accuracy with RMSE of 3.9157 whereas the LSTM has RMSE of 5.6121. A perfect prediction model based on the BER and adaption parameter is also presented. The perfect predictor model outperforms both the machine learning models and has a data rate of 2.7867, followed by the neural network with a data rate of 2.3391. However the design is not a sustainable one as it will soon be outdated due to increasing data rate demands. The data rate of the codec can be improved by using a more robust encoding such as Turbo codes and transmitting using more antennas. The codec can also be made to transmit a variety of different data types such as random packets and images.

TABLE OF CONTENTS

LIST OF FIGURES

LIST OF TABLES

1 Introduction

With the increasing number of internet users, more and more people are now sharing and consuming multimedia across the internet. It is therefore important to ensure that the end user has a smooth experience whilst interacting with media over the internet on a wireless network. A codec is one technique that enables users to interact with high quality media at a reasonable speed. A codec is defined as a software program that encodes and decodes a digital data stream. Different codecs are suited for different situations, these may be downloading and uploading, media playback or real time applications such as streaming and video conferencing.

In this work we aim to develop a machine learning based codec for a Wi-Fi router operating over a Raleigh fading channel. Essentially the codec is achieved by employing an adaptive modulation and coding scheme (AMC) to accommodate varying signal strengths. AMC enables a wireless network to dynamically select modulation and coding schemes (MCS) based on channel conditions in order to meet certain performance requirements. However it does not provide adaption capabilities for all channel conditions. The presented system is designed and simulated using MATLAB. MATLAB is selected as a simulation medium because it provides most implementations for the elements needed in this project.

This paper is organised as follows. The fundamental concepts of a wireless network, MIMO, AMC and existing solutions are presented in Section 2 . In Section 3 we give the requirements, constraints and success criteria for this project. Section 4 gives a detailed design methodology for the AMC model. The AMC results and critical decision is done in Section 6 . The project impact and sustainability are discussed in Section 8 and 7 .

2 Background

Wireless networks have gained popularity due to their expandability, accessibility and adaptability. Many people access the internet through a wireless network mainly WiFi. There is also a rising number of applications that now designed around WiFi access, these include: smart homes, smart cities, robotics and healthcare wearables. This has meant that wireless networks are usually congested due to increased data traffics and down time [1] [2]. There are no licence fees required to operate WiFi equipment, however there are protocols that dictate how such devices should operate. These protocols are developed by the IEEE under the 802.11n family. The 802.11n protocols specify the operating data rates and frequency band. WiFi uses a half-duplex connection operating on the physical layer on the ISO reference model. WiFi uses radio waves as a medium for transmitting information as such it suffers from issues such as access interference, path loss, shadowing and fading.

2 .1 Digital Communication Model

Wireless networks utilise a digital communication model. Digital communication systems generally outperform their analog counterparts. Digital systems are much cheaper to implement and well suited for long distance transmission. This project adopts the communication model depicted in Figure 2. Compression or source coding is the mapping from one sequence to a shorter sequence whilst minimising information entropy. Compression is needed in order to reduce file size without significant loss of information. Encryption is introduced in communication systems in order to make it hard for eavesdroppers to decipher transmitted information. Most digital communication systems use the Advanced Encryption Standard to introduce confusion and diffusion to a message. Forward error correction (FEC) is a means of implementing error control capability in communication systems. The transmitter introduces

redundant information to the information to transmitted. The receiver then automatically performs error correction of the received information. Given a message containing k bits the encoder appends r parity bits to add redundancy. The encoder then maps the message into a unique n bitstream, such a FEC is said to have a code rate of k/n. Commonly used FEC codes include Convolutions Codes, Turbo Codes, LDPC, BCH and RS codes.

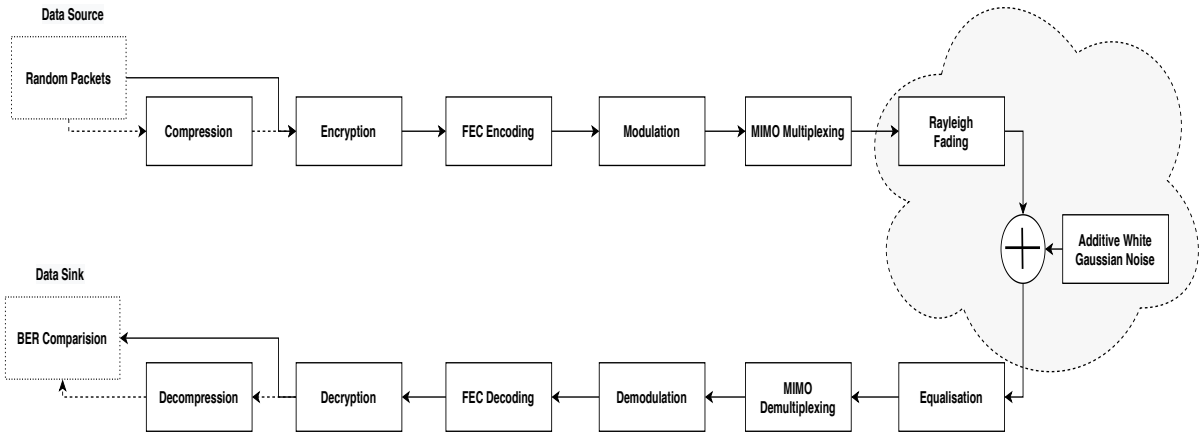

Fig. 1: Digital communication model.

Digital modulation performs a mapping from a bitstream to a signal waveform. The mapping is done using a parameter or a combination of parameters of the carrier signal. The most common types of digital modulation are Phase-shift keying (PSK), Frequency-shift keying (FSK), Amplitude-shift keying (ASK) and Quadrature amplitude modulation which is a combination of PSK and ASK. A M-ary modulation system is capable of transmitting 2^b unique waveforms at a given instance, where b represents coded bits.

2 .2 MIMO Systems

Multiple-Input Multiple-Output (MIMO) make use of multiple transmitter (Tx) and receiver (Rx) antennas. MIMO systems are used in wireless networks to improve channel capacity by decomposing a waveform and transmitting it using Tx independent channels. MIMO systems generally achieve higher spectral efficiency at a lower energy per bit. MIMO can also improve Signal-to-noise ratio (SNR) by using non-correlated antennas.

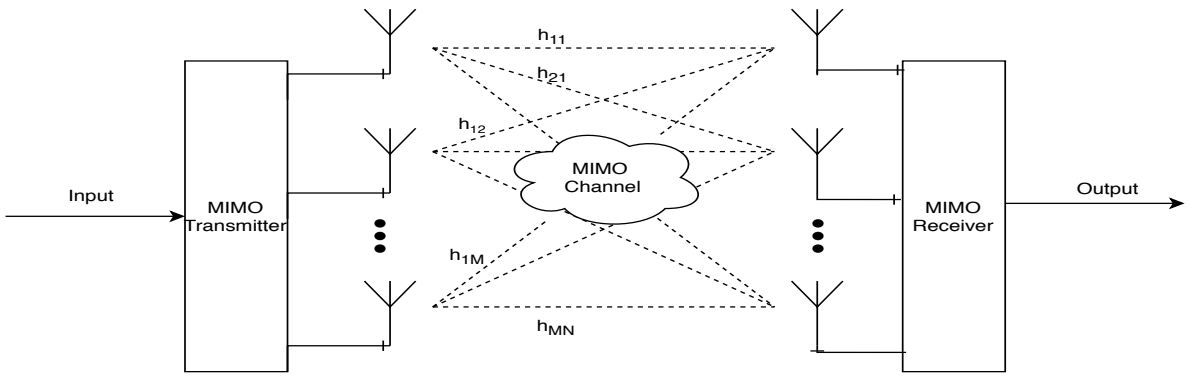

Fig. 2: MIMO structure with M transmitters and N receivers.

A narrowband channel can be modelled using a channel matrix [3] $\mathbf{H}$, where $\mathbf{H} \in \mathbb{C}^{N \times N}$ and $N = \text{Tx}$. The elements of the channel matrix represent amplitude and phase shift introduced by the channel. Element h_{ij} in $\mathbf{H}$ represents the channel connections between the i^{th} receiver antenna and the j^{th} transmitter antenna.

$$\mathbf{y} = \mathbf{H}\mathbf{x} + \mathbf{n} \tag{1}$$

where $\mathbf{y} \in \mathbb{C}^{N \times 1}$ denotes the output signal from the antennas, $\mathbf{x} \in \mathbb{C}^{N \times 1}$ the input signal to the MIMO and $\mathbf{n} \in \mathbb{C}^{N \times 1} \sim \tilde{\mathcal{N}}(0, \sigma^2)$ the channel noise vector. That is the channel noise is modelled as an independent complex additive white Gaussian noise (AWGN) random variable with zero mean. [4] indicate that capacity and spectral improvements by MIMO depend on channel state information (CSI) being available on both the transmitter and receiver, channel SNR and the correlation between channel gains of the antennas. [5] define the channel capacity of an uncorrelated MIMO antennas using the equation below assuming CSI is available at Tx and Rx.

$$C_{MIMO} = \log_2(\det[\mathbf{I} + \frac{\gamma}{\text{Tx}}(\mathbf{H}^{\mathbf{H}}\mathbf{H})^{-1}]) \tag{2}$$

where γ is the SNR at the receiver, $\mathbf{I}$ is an identity matrix with the same dimensions as $\mathbf{H}$ and $\mathbf{H}^{\mathbf{H}}$ is the Hermitian transpose of $\mathbf{H}$.

2 .3 Rayleigh Channel Fading

To model a Rayleigh fading channel the elements of $\mathbf{H}$ are assumed to be zero mean circularly symmetric complex Gaussian random variables with a unit variance. A complex Gaussian random vector $\mathbf{v}$ is circularly symmetric if its distribution is the same as $\mathbf{v}e^{j\theta}$ for any $\theta \in [0, 2\pi]$ [4]. A Rayleigh fading channel is more a appropriate model for wireless channels. This is because there is no direct path between the transmitter and receiver. Rayleigh distribution has been shown to accurately model such scenarios where there in no dominant line-of-sight transmission [6].

2 .4 Receiver Equalisation

Before the MIMO receiver, a zero forcing equaliser (ZF) is used to eliminate intercarrier and intersymbol interference introduced by the channel. A simple ZF can be described using equation 3. The ZF applies the inverse of the channel frequency response on the received signal [6]. The equaliser $\mathbf{W}$ is given by the equation below.

$$\mathbf{W} = (\mathbf{H}^{\mathbf{H}}\mathbf{H})^{-1}\mathbf{H}^{\mathbf{H}} \tag{3}$$

Where $\mathbf{W}$ is a complex matrix with dimensions the same as $\mathbf{H}$. The side effect of ZF is that it amplifies noise caused by linearly dependent columns [3]. ZF also fails to work if $\mathbf{H}^{\mathbf{H}}\mathbf{H}$ is singular.

A minimum mean square error (MMSE) detector is an alternative to a ZF detector. MMSE detector introduces a regularization term $\lambda = \sigma^2$ which makes it less sensitive to channel conditions [3].

$$\mathbf{W} = (\mathbf{H}^{\mathbf{H}}\mathbf{H} + \lambda\mathbf{I})^{-1}\mathbf{H}^{\mathbf{H}} \tag{4}$$

The advantage of using MMSE is that is applicable to both systems where $Tx > Rx$ and $Tx < Rx$ [3]. The remaining receiver elements perform inverse operations of their respective transmitter counterparts.

2 .5 Adaptive Modulation and Coding

Adaptive modulation and coding is a topic of much interest within the field of telecommunications with several already existing solutions. [7] use SNR based adaption using MPSK and RS codes. They switch between schemes using a channel predictor given by $SNR_1 = \alpha^2(SNR)$ where SNR_1 is the SNR value determined by the transmitter and α is the fading amplitude. Their results show that fixed rate codes achieve better BER in Rayleigh fading. In [8] they present a design that takes into account the medium access control performance requested by an application. They use M-QAM with punctured convolutional code bounds described in [9]. [8] uses a MMSE and channel prediction model defined as $\hat{\mathbf{H}}_{next} = \mathbf{H}_{current} + \frac{L_{current}}{L_{prev}}\Delta\mathbf{H}$, where by $L_{current}$ and L_{prev} represents the length of current and previous packet length and $\Delta\mathbf{H}$ is the difference between the current and previous channel matrices. The paper by [8] show that the output decoder performance can be modelled using code rate and pre-decoder uncoded BER. [10] incorporate practical considerations such as hardware specifications and pulse shaping. Their model is based on power and BER constraints using trellis codes. A more robust algorithm is presented in [11] which takes IEEE 802.11n guard interval sizes into consideration. In the paper they derived the optimal BER value for switching between the MCS's and conclude that their algorithm provide high throughput whilst being reliable. The basis for many AMC systems is SNR estimation for varying channel conditions where by receiver requires CSI for a successful AMC.

Using a fully connected neural network (NN) and a convolutional neural network [12] has been able to get better results that traditional AMC designs for 64QAM using MMSE. The AMC model by [13] uses supervised learning to reduce complexities and a deep neural network for channel estimation using channel matrices as training data. In this design each channel matrix is mapped to its respective transmitter antenna. Results from [13] show that such a design outperforms conventional designs whilst being less complex. [14] deployed a model that achieved an accuracy of 50% using trace logs as training data. [14] use a classification NN with a single hidden and the type of MCS neurons in the output layer. Su et al in [15] use reinforcement learning based AMC for underwater communication, their design reduces BER with less energy consumption. [16] explores a NN channel prediction model under different channel models namely Jakes, Clarke/Gan's and 3GPP Spatial Channel Model. Their model perform batter when using Jakes model because of the strong time domain correlation in Jakes over different SNR values. In order to improve performance and system reliability [17] suggests an online learning algorithm for AMC that keeps a database of post performances. This approach allows the training data to be generated whilst the system is in use. The advantage to this is that the model is updated as the channel conditions change as a result accuracy and reliability are also improved.

3 Design Considerations

In order for the proposed design to be a practical and feasible implementation, certain design decisions are taken based on following components.

3 .1 Requirements and Constraints

The main constraints imposed on this project are that the planning and execution should be done as an individual, and that the project should be completed within a span of 5 weeks. The design is expected to

meet the following requirements:

- The codec must achieve a rate of at least 2 bits/Hz.
- Raleigh fading channel with a bandwidth of 4MHz.
- The data rate must be at least 10Mbits/s.

3 .2 Assumptions

To reduce the complexity and scope of this work, the following assumptions are made in developing the AMC simulation.

- The channel is quasistatic which means that the fading coefficients stay constant for the entire codeword.
- Both the transmitter and receiver are stationary.
- CSI is known at the receiver antenna, as such there is no feedback channel needed.
- The antennas are independent from each other, that is the channel has unique channel coefficients for each antenna.
- The data to be transmitted has been compressed and encrypted.
- Hardware exists to support the proposed codec.

3 .3 Success Criteria

The success of the project is mainly dependent on designing a simulation model that meets the aforementioned requirements and constraints. Furthermore the proposed solution should be sustainable, and address social, economic and environmental aspects related to its development. The type of MCS, MIMO architecture and machine learning model should be justified is the design process as well as parameter choices.

4 Codec Adaptive Modulation and Coding Model

The simulation is run at a frame level, with each frame consisting of a sequence of randomly generated bits. We use BCH codes with symbols from binary filed $GF(2^m)$ where $m = 4$. The encoder used is a BCH with message length $k = 5$ and codeword length $n = 2^m - 1 = 15$ that is capable of correcting up to 3 errors, given by $t \geq \frac{n-k}{m}$. As a result the stream is encoded at a rate of $1/3$. BCH codes are chosen over other simple codes such as RS codes because of better performance over fading channels as shown in [18].

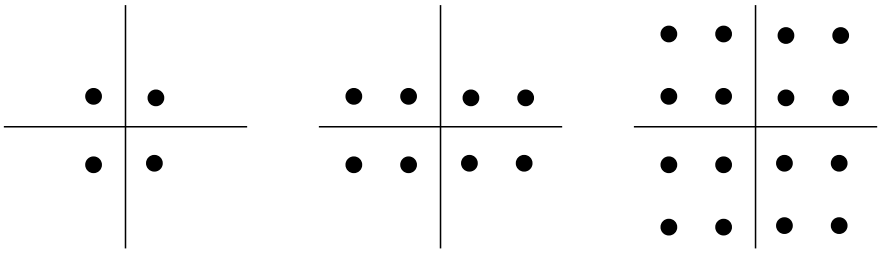

(a) 4QAM (b) 8QAM (c) 16QAM

Fig. 3: An illustration depicting the constallations for the QAM signal at different modulation levels. The constallations is in signal space.

The modulation scheme used in this project is QAM. QAM utilises both ASK and PSK, as such it provides better spectrum efficiency than any of them separate. Figure 3 shows the constellation for QAM at the chosen modulation levels.

In order to increase channel capacity and spectral efficiency the proposed AMC uses MIMO multiplexing. The AMC makes use of a 2×2 MIMO, this is $Tx = 2$ and $Rx = 2$. Equation 1 can be rewritten as Equation 5 for simulation purposes. Equation 5 shows the exact structure adopted in the code.

$$\begin{bmatrix} y_1 \\ y_2 \end{bmatrix} = \begin{bmatrix} h_{11} & h_{12} \\ h_{21} & h_{22} \end{bmatrix} \begin{bmatrix} x_1 \\ x_2 \end{bmatrix} + \begin{bmatrix} n_1 \\ n_2 \end{bmatrix} \tag{5}$$

Three different MCS are used in the simulation. These subsystems are combines to make up the AMC, Table 1 shows the structure for each MCS. MCS1 is the only one that does not make use FEC.

Table 1: Modulation and coding schemes for the AMC.

MCS	**Code rate**	**QAM order**	**MIMO**	**SE**	**E$_s$**
MCS1	1	4	2×2	4	2
MCS2	1/3	8	2×2	2	6
MCS3	1/3	16	2×2	2.67	10

The MCS parameters are chosen such the each of them meets the requirements defined in Section 3 .1. Using Equation 6 it can be shown that the selected MCS meet the 2 bits/Hz rate. Using a pulse shaping coefficient of $\alpha_p = 1$, MIMO coefficient $\alpha_m = 2$, M being the modulation order and R representing the FEC code rate. MCS1, MCS2 and MCS3 have spectral efficiencies of 4 bits/Hz, 2 bits/Hz and 2.67 bits/Hz respectively.

$$SE = \frac{R\log_2(\mathrm{M})\alpha_m}{\alpha_p} \tag{6}$$

The AWGN is generated at the beginning of each frame. The noise variance σ_n^2 is dependent on SNR (γ) and the MCS used. The noise variance for each MCS can be determined using Equation 7.

$$\sigma_n^2 = E_s \frac{n}{k\log_2(\mathrm{M})} 10^{(-\frac{\gamma}{10})} \tag{7}$$

Where E_s is the average energy of the symbols after modulation. The energy can be computed by taking the mean of the distances squared of the constellations. The average energies for 4QAM, 8QAM and 16QAM are 2, 6 and 10 respectively.

$$C_{n,k} = \frac{n}{k} F \tag{8}$$

$$S_M = \frac{C_{n,k}}{\log_2(\mathrm{M})} \tag{9}$$

$$S_{MIMO} = \frac{S_M}{Tx} \tag{10}$$

The frame structure of the simulated packets is described using Equation 8 - 10. Where F is the frame size, $C_{n,k}$ is the number of coded by bits from an (n, k) encoder, S_M are the symbols from a M-ary modulator and S_{MIMO} are symbols from each antenna. The simulation uses a frame size of 2000 bits for each MCS. Table 2 shows the frame structure for each of the MCSs.

Table 2: Modulation and coding schemes frame structure.

MCS	**Coded bits**	**QAM symbols**	**Antenna symbols**
MCS1	2000	1000	500
MCS2	6000	2000	1000
MCS3	6000	1500	750

We use a MMSE equaliser based on the reasons already discussed in Section 2 .4 to remove errors introduced by the channel. The output signal $\mathbf{x}'$ from the MMSE equaliser is defined using Equation 11. In order to recover the transmitted signal $\mathbf{x}$, the respective inverse operations are performed on $\mathbf{x}'$ as illustrated in Figure 2.

$$\mathbf{x}' = \mathbf{W}\mathbf{y} \tag{11}$$

In order for the proposed model to be adaptive to channel conditions a recursive model is provided in Equation 12 that relates the current channel $\mathbf{H_f}$ to the previous frame channel $\mathbf{H_{f-1}}$. Equation 12 models a discrete channel update, it follows that the channel update can be written as a ARMA process which can be used to model the correlation in a linear discrete process.

$$\mathbf{H_f} = \alpha\mathbf{H_{f-1}} + (1 - \alpha)\mathbf{G_f} \tag{12}$$

The extent to which the channel is correlated is controlled by $\alpha \in (0, 1)$ which is the fading steady state coefficient. A large α means a high channel correlation and a lower one means low channel channel correlation. The parameter $\mathbf{G}_f$ is used to introduce random channel errors using conditions states is Section 2 .3. The channel starts to fade from the second frame as such $\mathbf{H_f}$ is initialised to an identify matrix for the first frame. $\mathbf{H_f}$ and $\mathbf{G}_f$ are determined at the end of frame.

We define the adaption parameter ζ which is a measure of the effect by the channel and equalizer to the SNR. The adaption parameter is used to specify the range at which a given MCS is active. The adaption parameter given a measure of the effect of the channel and equalizer $\mathbf{Z} = \mathbf{HW}$ to SNR.

$$\zeta = \frac{\sum_{i=1}^{N}\sum_{j=1}^{N}(|\mathbf{Z}_{ij}|)^2}{\sum_{i=1}^{N}\sum_{j=1}^{N}(|\mathbf{W}_{ij}|)^2} \tag{13}$$

A translation is done from the SNR VS BER curves to a set of ranges in ζ. The translation rule is the most spectral effective MCS should be active for majority of the frames. Using the model in Equation 12 it can be shown that ζ has a variation centered at the initial value of $\sum_{i=1}^{N}\sum_{j=1}^{N}(|\mathbf{H}_{ij}|)^2$.

5 Machine Learning Based Predictor

Machine learning particularly neural networks have the ability to model complex functions without explicit programming. A closed form AMC predictor will have superior performance compared to a machine learning based predictor. However it does not generalize well to unknown channels. The class of machine learning adopted for proposed AMC predictor is known as supervised learning. In this class the machine learning model is expected to use training data to build a function mapping inputs to outputs. Training data is generated by the simulation. The NN uses regression supervised learning to predict the next ζ value which is used to decide which MCS to switch to in the next frame.

The neural network takes the training data $\mathbf{x}$ a column vector in the input layer. The parameters associated with a NN are usually real and positive. During forward propagation the hidden layer takes the the outputs $\mathbf{a}^{l-1}$ from the previous layer process it then pass it to successive layer. This process continues until the output layer. The neural network operations are described in vector notation.

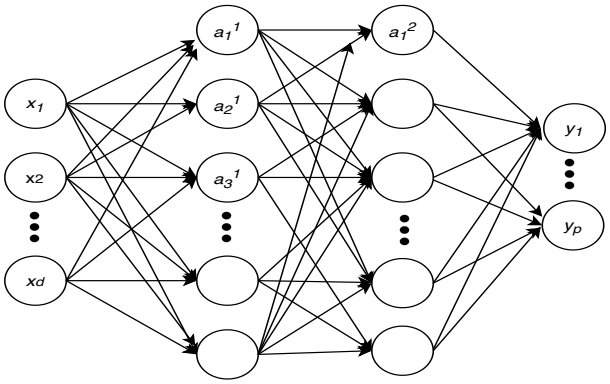

Fig. 4: Simple neural network structure with two hidden layer, $\mathbf{x}$ representing d input samples and the prediction value as $\mathbf{y}$ with p output samples.

An activation function used to decide which neurons should be active during forward propagation. A neuron in layer l will be active if $\mathbf{a}$ is greater than some threshold value. Equation 14 is used to determine the action for neurons in layer hidden layer l. In general the activation function σ is non-linear function, where $\mathbf{b}^l$ is the bias row vector for neurons in layer l and $\mathbf{W}^l$ is the weight matrix for weights between layer l and $l-1$.

$$\mathbf{a}^l = \sigma(\mathbf{b}^l + \mathbf{W}^l \cdot \mathbf{a}^{l-1}) \tag{14}$$

The operator $\cdot$ is used to denote the dot product between two matrices. The Sigmoid, Softmax, ReLu are some of the most commonly used activation functions. The weight is proportional to how much contribution the neuron in the previous layer has to the neuron in the next layer.

The accuracy of the neural network is determined at the end of each forward propagation epoch or iteration. The cost or loss function $\mathcal{L}$ is used to determine the difference between the predicted value $\hat{\mathbf{y}}$ and the expected value $\mathbf{y}$.

Forward propagation is not enough since it is a one way process used to get prediction values. The actual training of the NN is done through a process known as Backpropagation. Backpropagation is used

optimise $\mathcal{L}$ such that the error is minimum. Backpropagation using gradient descent aim to find the global minima of $\mathcal{L}$, as it represent the state when the NN has minimum error. Gradient descent computes the derivative of the cost function respect to the parameters of interest in this case the weights and biases.

Equation 15 and 16 provide the update rule for adjusting the weights and biases for neurons in back-propagation. The learning the rate η is the step size between points at which the gradient is computed. The learning rate should be set such that the model converges to a local minima at a reasonable rate. Generally there is a trade off between accuracy and generalisation of a model. The model should capture the fundamental relationship without capturing outliers of a dataset. The model should be able perform at comparable accuracy when given unseen data.

$$w' = w - \eta \frac{\partial \mathcal{L}}{\partial w} \tag{15}$$

$$b' = b - \eta \frac{\partial \mathcal{L}}{\partial b} \tag{16}$$

The second proposed predictor is using a Long Short-Term Memory (LSTM) which is a variant of a Recurrent Neural Networks (RNN). RNN allow information to persist in the neurons. This is in contrast to the a simple NN which only depends on the current input. LSTM allow a RNN to long term dependencies in data. LSTM contain structures called memory cell which modify the information in network. The information flow in a memory cell in controlled by gates. The forget gate is used to discard information no longer needed by the memory cell. The input gate dictate when new information is added to the memory cell and the output is responsible for determining the output based on input data. The operations used in a LSTM are similar to those in a traditional NN with slight variations in order to accommodate for additional computational units. Detailed LSTM operations are described in [19].

5 .1 Predictor Design

The NN used in this project is for regression. The NN is trained a train with a window size of 4. This means that each 4 ζ points are needed to predict the next value of ζ. The value of the predicted ζ will be used to select to a specific MCS used in the next frame. The the rest of the structure such as number of hidden layers, learning rate and others are determined through experimentation. A similar approach is used for the LSTM. The finally parameters are chosen such that the output from the loss function in minimum. Both predictors use Root Mean Square Error (RMSE) as a loss function, calculated using Equation 17 over n data points. MCS classification is done using the ζ values determined by the predictor by using the of the range of ζ values which were previously determined in Section 4 .

$$RMSE = \sqrt{\sum_{i=1}^{n} \frac{(\hat{y} - y)^2}{n}} \tag{17}$$

6 Simulation Results and Analysis

The simulation results can be reproduced using the listed code in Appendix E. The first task carried out what determining the modulation orders for the different MCSs. Figure C.1 and Figure C.2 - Figure C.4 are used to decide the QAM levels used in the simulation. The plots show the SNR vs BER curves

for the MCSs in a non fading channel without AWGN, we observe that spectral efficiency is inversely proportional to modulation. We expect the spectral performance to be similar when fading is included. Initially the simulation is run in order to determines the effective ζ and SNR regions for each MCS.

Using Equation 12 we see that if α is close to a value of 1 then the channel is almost perfectly correlated since the noise term $\mathbf{G}_f$ will have negligible effect on the channel conditions in the current frame. Figure D.3 shows a high correlation, we observe that shows an almost linear relationship between 10logζ and the frame progression. A small α means that the channel in uncorrelated and the noise term has significant effects on channel. This can be seen in Figure D.4 where ζ has a large variation between successive frames. The α value is chosen such that it strikes a balance between the two extremes. Ultimately we set on $\alpha = 0.96$ and $\sigma_g^2 = 3$. The channel variance σ_g^2 is kept constant in order to make comparison simpler. The specific value of σ_g^2 was experimentally determined through an iteration process. Figure 5 shows ζ with the chosen channel model parameters settles on.

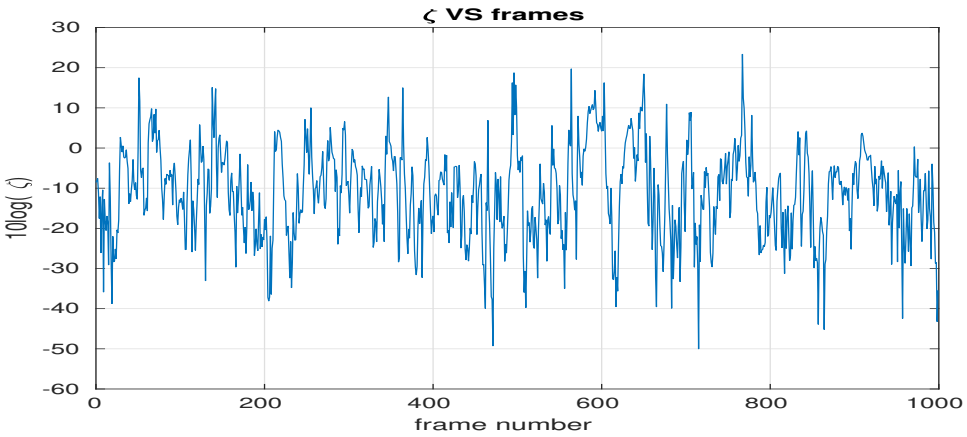

Fig. 5: Low correlation $\alpha = 0.96$ and $\sigma_g^2 = 3$.

Using Figure 5 the MCS regions are define to be MCS1 for $\zeta \in [0, \infty)$, MCS2 for $\zeta \in (0, -15)$ and MCS3 for $\zeta \in (-\infty, -15,]$. Further more we observe that the value of 10log(ζ) are centred around 10log$(\sum_{i=1}^{N} \sum_{j=1}^{N} (|\mathbf{H}_{ij}|)^2) = 0$, which can seen more clearly in Figure 8 with most points saturated around the horizontal axis.

Table 3: MCS operational range

	ζ **range**	**SNR range**
MCS1	$[0, \infty)$	$(-\infty, 32]$
MCS2	$(0, -15)$	$(32, 37)$
MCS3	$(-\infty, -15,]$	$[37, \infty)$

The table below shows the operating ranges for each MCS system. These ranges are used to by the predictor decide on which MCS to employ at a give frame.

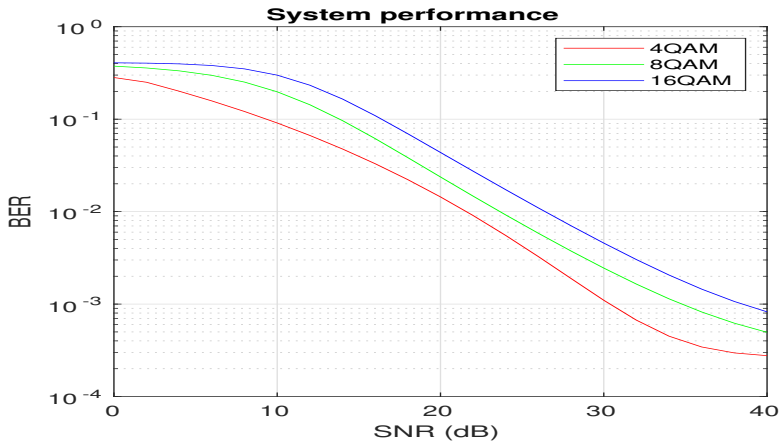

Fig. 6: SNR vs BER curves for the selected MCS at $\alpha = 0.96$ and $\sigma_g^2 = 3$.

The SNR at which the received signal experiences significant BER curves are shifted to the right by a factor of $10\log(\sum_{i=1}^{N}\sum_{j=1}^{N}(|\mathbf{W}_{ij}|)^2)$ due to the fact that steady state coefficient fading is less that 1 therefore. The curves generated in this figure are are used determine the BER threshold for the AMC. We select a BER threshold of 10^{-3} which means 100 error bits for every 100, 000 transmitted bits. The effective AMC SNR ranges can then determined using the BER threshold and MCS ζ regions as scaling conditions. The mean $\zeta = -11$, which is determined through the simulation corresponds is translated to a SNR value of 30db which is the point at which the left most curve meets the BER threshold. The SNR regions are then defines to span a proportional regions to ζ. The regions are defined to be MCS1 for SNR $\in (-\infty, 32]$, MCS2 for SNR $\in (32, 37)$ and MCS3 for SNR $\in [37, \infty)$.

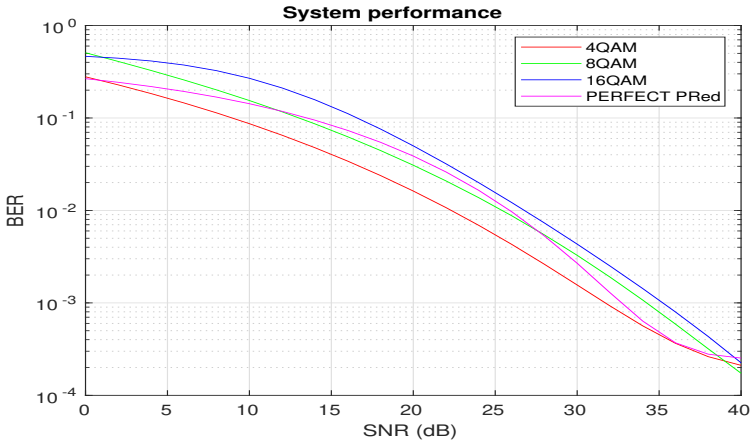

Fig. 7: Perfect AMC predictor

The perfect predictor is developed to be the most optimal AMC. It predicts the channel conditions by calculating the ζ for the next frame and then selecting the appropriate MCS based on that value. As such the perfect predictions is able hop to the optimal MCS for a given frame. The perfect predictor in bounded by the 4QAM and 16QAM as expected with a shape that maximises the effective data rate.

The machine learning data set if generated by obtaining Figure 5 and Figure 6. The data set is slit such that 90% is used for training and the rest as testing data. Each of the predictors also give the

MCS classifications for each ζ. The specify parameters for used for the neural network and LSTM were empirically determined.

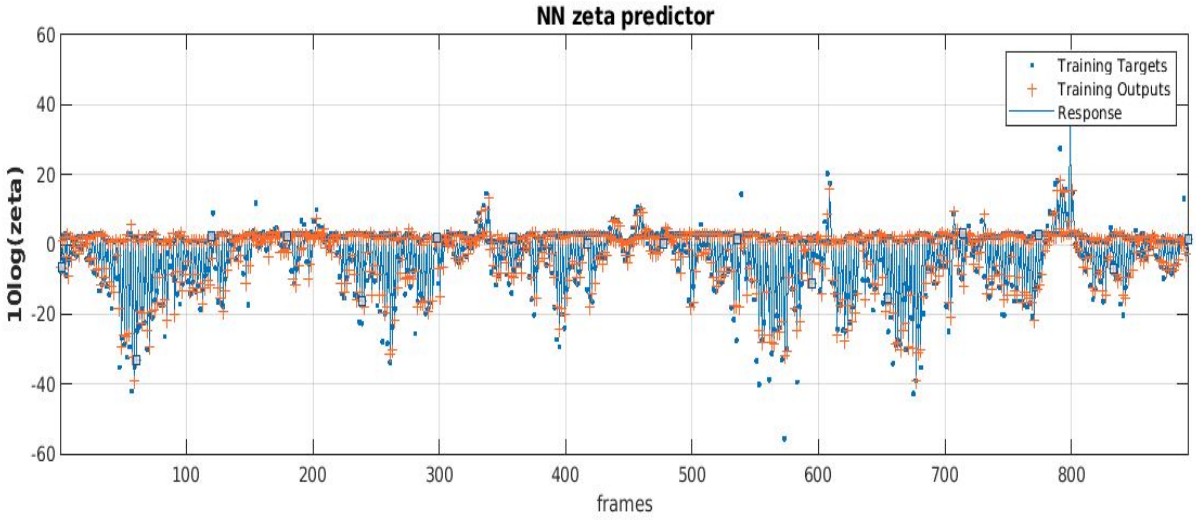

Fig. 8: Neural network predictor.

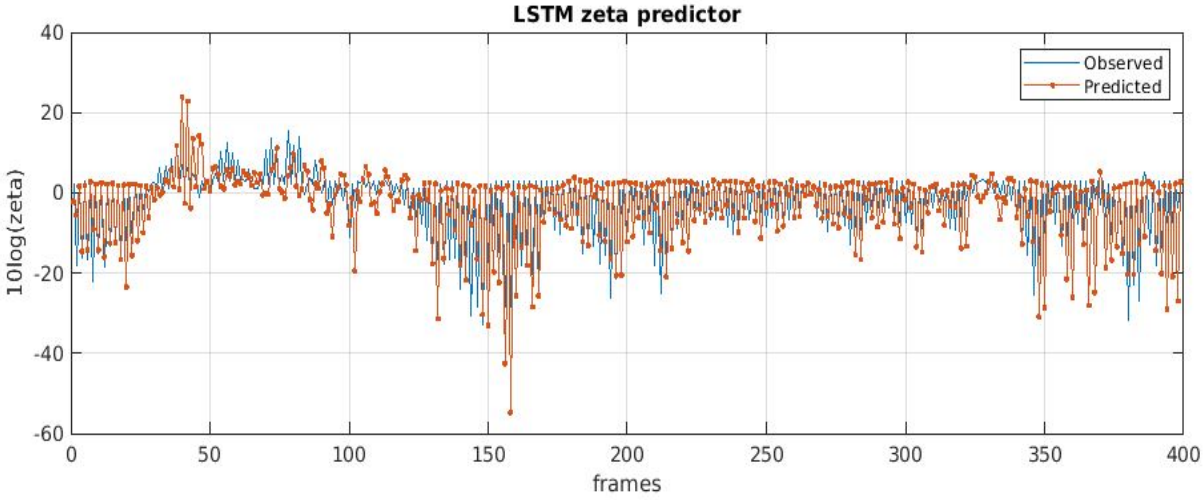

Fig. 9: Long short term memory predictor.

The predictor's AMC performance is determined by computing the effective data rate of each system. The data rate is calculated as $R_b = Tx(BER_t)\sum(R)(FM)log_2 M$. Where M is modulation order of the MCS, R is its code rate, FM is the number of frames the MCS is active, and (BER_t) is the BER threshold for the AMC. The data rates for the AMC predictors is shown in the table below.

Table 4: Data rates from AMC implementations.

	MCS1	**MCS2**	**MCS3**	**Data Rate**
Perfect Pred	252	325	424	2.7867
NN	104	267	521	2.3393

The data rate for the LSTM is not included because it was only tested with the first 200 frames. This results in the data rate of the LSTM to be significantly lower compared to the other two. The reason for this is the beginning frames tend to use more 4QAM as seen in Figure 7 where the perfect predictor is bounded between 4QAM and 8QAM for the first 10 SNR values. The LSTM has to be run over a comparable number of frames as the other predictors in order to be able to perform an accurate statistical comparison. However can reach a conclusion by considering the RMSE for each of the systems since both predictors were trained using the same amount of data. By definition the RMSE for the perfect predictor is 0 whereas the NN and LSTM have a RMSE values of 3.9157 and 5.6121 respectively. From this we can conclude that the perfect predictor is more accurate followed by the NN predictor and lastly the LSTM. The prefect predictor is 16% more efficient that the NN predictor.

The effects of σ_g^2 and α on the data rate are also evaluated in the simulation. The graph below shows the data rate a function of σ_g^2 and α.

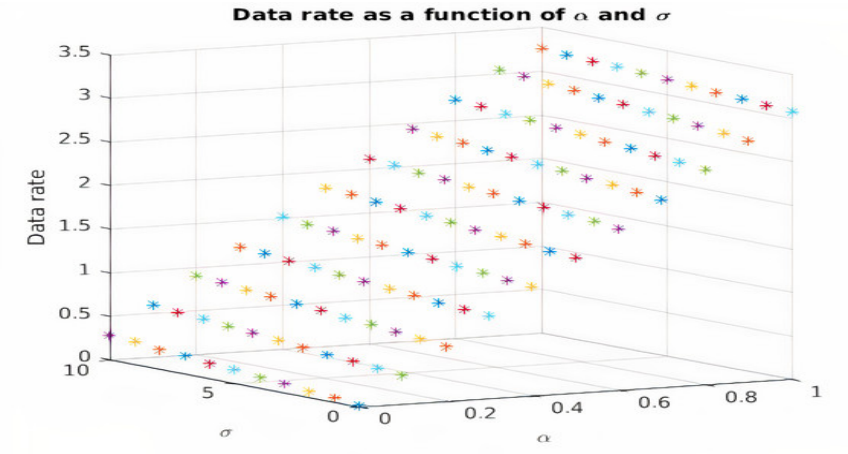

Fig. 10: The effects of α and σ_g^2 on the data rate.

The graph shows a positive linear relationship between the 3 parameters. Based the results presented in this section the project is deemed a success as it meets the design requirements mentioned in 3 .1.

7 Impact

It is important to identify and evaluate the impact an engineering solution in order to ensure that it is a holistic design and that unintended consequences of the design are recognised and addressed. The design is evaluated across fields discussed below.

7 .1 Environmental

WiFi routers are mostly constructed from plastic and other recyclable components therefore their e-waste contribution is reduced. However the manufacturing process used to produce plastic usually has negative impacts environmental. Plastic is made from oil, the process of converting oil into plastic is energy demanding and most manufacturing plants burn coal as an energy source. Further more not all kinds of plastic are recyclable and oil spills are a huge environmental hazard. Communication systems also reduce the carbon footprint since they provide a means of remote communication.

7 .2 Social

Wireless communication made it easier and cheaper to access a global audience. People are now able to keep in contact even when far apart. Many developing countries access the internet through wireless network. This is because WiFi routers are potable and cheaper compared to fibre [20]. Communication is one of the defining constructs of human societies. Therefore WiFi as a communication method has the ability to alter existing social structures [21]. The social impact of communication system can seen in the current pandemic where majority of social interactions occur remotely due to social distancing.

WHO indicates that there has not been any medical cases that are as a result of exposure to WiFi signals as of date [20]. A study by [22] supports this claim, by examining previous WiFi studies they conclude that most of them were poorly conducted and thus presented flawed results. Wireless communication makes it easy to consume multimedia as a source of entertainment. The side effect of this is that it may result in health conditions associated with a lack of exercise or movement and eyesight problems due to prolonged screen time.

7 .3 Economic

Remote communication means business can coordinate operations across different time zones. This means business can conduct more business and individuals have access to more opportunities by working remotely. Wireless communication systems remove the cost barrier to acquiring new information many institutions and sites provide open access educational resources. Individuals and small companies are now able to compete with large corporations because they can conduct business without having physical offices. Wireless communication can cut down a business operating costs by reducing the budget spent on travelling costs [21]. This kind of communication encourages a competitive market since clients have access to a large pool of options. A study by [23] shows that 1% increase in ICT infrastructure can result in a GDP per capita growth between 0.0767% for broadband subscriptions and 0.396% for mobile.

8 Sustainability

A sustainable engineering solution is one that meets current requirements whilst accounting for future demands. The design should not make use of limited resources, should be operational for a reasonable duration and have a positive impact. WiFi is expected to expand to the 6GHz spectrum. This is a move that is aimed at proving faster, reliable and wider network coverage. This is in response to the growing number of WiFi devices. Typical WiFi networks use the 2.4GHz and some at the 5GHz band. The frequency at which device's network operates is limited by the router [24]. The 2.GHz band tends to have a wider coverage and better at passing through obstructions compared to 5GHz [25]. However 5GHz is more faster than 2.4GHz band. There are more interferences in the 2.4GHz band due to the large number of devices utilising this band making it more unreliable and congested.

The proposed solution is a software based codec with only the antennas as physical components. This means that the system can easily be updated without additional costs to the user. The limiting factor is the hardware which goes obsolete when new and improved one is developed. The energy consumption of the proposed solution is minimised by using a 2×2 antenna configuration, which has the least number of antennas needed for MIMO. It usually takes a couple of years for device manufacturers to design devices that meet the latest standards, this means that the designed codec could be deployed for a couple of years before being absolute. Essentially the presented solution will not be able to compete with routers operating in higher bands when devices migrate to newer standards. However the presented solution will

be able to serve most users in the meanwhile operating at the 2.4GHz band.

9 Project Management

To ensure that the project is completed in a timely and structured manner a project plan was created for the project. The project plan took into consideration the project scope, complexity and duration. The developed project plan is included in Appendix F. The project plan is used to assist the student to work effectively outside their designated design field group. Weekly meetings are scheduled by the supervisor with the group. The meetings are used to facilitate discussions around the design topic and provide guidance and support with regards to issues that may arise during the design process. The project required research, planning and implementation with an emphasis on computer simulation. As such an engineer's notebook is used to record meeting minutes and progress during the span of the project. The project outcomes and engineer's notebook can be found in Appendix B and Appendix G.

10 Future Recommendations

The current AMC is only simulated with fewer parameter variations due to time constraints. As a result we use a single type of data source, a fixed MIMO structure and the same FEC encoder. A future AMC can be designed that includes these variations. The AMC can improved by making use of more robust by FEC's such as Turbo codes. Further experimentation is needed to optimise the machine learning parameters and to explore several neural network architectures. The simulation could also be made to be time dependent in order to get more representative performance measurements. These recommendations can be used to design a codec with a higher data rate which would be a sustainable design solution compared to the current one.

11 Conclusion

This report presents the design and implementation of a machine learning based adaptive codec. The system is simulated under a Rayleigh fading channel. The designed codec uses 8QAM and 16QAM with a 1/3 BCH encoder and 4QAM without FEC. MIMO is incorporated into the design in order to increase spectral efficiency. Three different AMCs are implemented namely a perfect predictor, LSTM predictor and a NN predictor. The neural network model has a RMSE of 3.9157 whereas the LSTM has RMSE of 5.6121. The perfect predictor is a superior design with a data rate of 2.7867 and the NN coming second with a data rate of 2.3393. The project is deemed a success as it meets the specified design requirements. However the AMC design can be further improved by using a more robust encoding and modulation techniques. We also investigate the sustainability and impact of the presented codec. The codec is able to service users operating withing the 2.4GHz however it falls short in meeting future network demands. Therefore the current codec is not a sustainable design. It is however a maintainable one due to the fact that it is a software based codec.

Acknowledgement

I would like thank Prof Fambirai Takawira for his assistance and advice during the span of the project. I would also like to thank my design project group members for their fruitful discussions. The project was a fun and educational one, it helped me to get exposure to new concepts and engineering fields.

REFERENCES

[1] J. Chen, L. Zhang, Y.-C. Liang, X. Kang, and R. Zhang, "Resource allocation for wireless-powered iot networks with short packet communication," *Trans. Wireless. Comm.*, vol. 18, no. 2, p. 1447–1461, Feb. 2019. [Online]. Available: https://doi.org/10.1109/TWC.2019.2893335

[2] Y. . E. Wang, X. Lin, A. Adhikary, A. Grovlen, Y. Sui, Y. Blankenship, J. Bergman, and H. S. Razaghi, "A primer on 3gpp narrowband internet of things," *IEEE Communications Magazine*, vol. 55, no. 3, pp. 117–123, 2017.

[3] K. Rundstedt, "Measurements and channel modelling of microwave line-of-sight mimo links," 2015.

[4] A. Goldsmith, S. A. Jafar, N. Jindal, and S. Vishwanath, "Capacity limits of mimo channels," *IEEE J.Sel. A. Commun.*, vol. 21, no. 5, p. 684–702, Sep. 2006. [Online]. Available: https://doi.org/10.1109/JSAC.2003.810294

[5] S. Ahmadi, "Chapter 4 - new radio access physical layer aspects (part 2)," in *5G NR*, S. Ahmadi, Ed. Academic Press, 2019, pp. 411 – 654. [Online]. Available: http://www.sciencedirect.com/science/article/pii/B978008102267200021X

[6] F. Conillera Vilar, "Implementation of zero forcing and mmse equalization techniques in ofdm," 2015.

[7] K. M. S. Soyjaudah and B. Rajkumarsingh, "Adaptive coding and modulation using reed solomon codes for rayleigh fading channels," in *EUROCON'2001. International Conference on Trends in Communications. Technical Program, Proceedings (Cat. No.01EX439)*, vol. 1, 2001, pp. 50–53 vol.1.

[8] F. Peng, J. Zhang, and W. E. Ryan, "Adaptive modulation and coding for ieee 802.11n," in *2007 IEEE Wireless Communications and Networking Conference*, 2007, pp. 656–661.

[9] M.-G. Kim, "On systematic punctured convolutional codes," *IEEE Transactions on Communications*, vol. 45, no. 2, pp. 133–139, 1997.

[10] Soon-Ghee Chua and A. Goldsmith, "Adaptive coded modulation for fading channels," in *Proceedings of ICC'97 - International Conference on Communications*, vol. 3, 1997, pp. 1488–1492 vol.3.

[11] P. Patil, M. Patil, S. Itraj, and U. Bombale, "Ieee 802.11n: Joint modulation-coding and guard interval adaptation scheme for throughput enhancement," *International Journal of Communication Systems*, vol. 33, no. 8, p. e4347, e4347 dac.4347. [Online]. Available: https://onlinelibrary.wiley.com/doi/abs/10.1002/dac.4347

[12] B. Zhu, J. Wang, L. He, and J. Song, "Joint transceiver optimization for wireless communication phy using neural network," *IEEE Journal on Selected Areas in Communications*, vol. 37, no. 6, pp. 1364–1373, 2019.

[13] P. Yang, Y. Xiao, M. Xiao, Y. L. Guan, S. Li, and W. Xiang, "Adaptive spatial modulation mimo based on machine learning," *IEEE Journal on Selected Areas in Communications*, vol. 37, no. 9, pp. 2117–2131, 2019.

[14] M. Chamat and B. D. Kodra, "Machine learning based modulation and coding scheme selection," 2019.

[15] W. Su, J. Lin, K. Chen, L. Xiao, and C. En, "Reinforcement learning-based adaptive modulation and coding for efficient underwater communications," *IEEE Access*, vol. 7, pp. 67 539–67 550, 2019.

[16] R.-F. Liao, H. Wen, J. Wu, H. Song, F. Pan, and L. Dong, "The rayleigh fading channel prediction via deep learning," *Wireless Communications and Mobile Computing*, vol. 2018, pp. 1–11, 07 2018.

[17] R. C. Daniels, "Machine learning for link adaptation in wireless networks," 2011.

[18] F. Lone, A. Puri, and S. Kumar, "Performance comparison of reed solomon code and bch code over rayleigh fading channel," 07 2013.

[19] J. Brownlee, *Long Short-term Memory Networks with Python: Develop Sequence Prediction Models with Deep Learning*. Machine Learning Mastery, 2017.

[20] "What 6 ghz spectrum means for connectivity, key industries, and technology implementers," Jul 2019. [Online]. Available: https://go.abiresearch.com/lp-future-of-wifi

[21] J. E. Katz, "Social and organizational consequences of wireless communications: A selective analysis of residential and business sectors in the united states," *Telematics and Informatics*, vol. 14, no. 3, pp. 233 – 256, 1997. [Online]. Available: http://www.sciencedirect.com/science/article/pii/S0736585397000014

[22] M. L. Pall, "Wi-fi is an important threat to human health," *Environmental Research*, vol. 164, pp. 405 – 416, 2018. [Online]. Available: http://www.sciencedirect.com/science/article/pii/S0013935118300355

[23] E. Toader, B. N. Firtescu, A. Roman, and S. G. Anton, "Impact of information and communication technology infrastructure on economic growth: An empirical assessment for the eu countries," *Sustainability*, vol. 10, no. 10, p. 3750, 2018.

[24] T. Oldcommguy, "The current and future state of wifi bands and channels!" Jul 2019. [Online]. Available: https://www.networkdatapedia.com/post/2019/07/15/the-current-and-future-state-of-wifi-bands-and-channels

[25] C. Duckett, "Stop using 2.4ghz and rely on 5ghz wi-fi: Acma nbn modem study," Jul 2019. [Online]. Available: https://www.zdnet.com/article/stop-using-2-4ghz-and-rely-on-5ghz-wi-fi-acma-nbn-modem-study/

APPENDIX A Non-Technical Report

THE TECHNOLOGY THAT DRIVES YOUR DIGITAL LIFE

1 Introduction

It is uncommon these days to meet someone without a mobile device or someone who hasn't used one. Most people reading this article are doing so through their screens. This is power that the mobile device puts in our hands. Gone are the days where you needed to needed to burn oil in order to deliver an important message. The mail is simple too inefficient for the new world where opportunities arrive and disappear within minutes. Landline phones limit your experience because they do not provide context that pictures or videos does.

2 Impact of Wireless Networks

Wireless networks solve all these problems. It gives you the ability to text and video call your friend across the world without having to be at a fixed location to do so. This opens a world of possibilities. Wireless communications means you are no longer limited by your physical location. It also means that you are able to get news faster and make decision much quicker. The internet means that there are multiple sources of information such as social media and blogs as such it is hard to mislead people over the internet because it is easy to fact check. Wireless communication provide easy ans simple access to the internet. The internet is a database of human experiences where everyone can append their own. Such a database means ones does not have to experience situations first hand in order to appreciate them since each individual has no limit to what they can or cannot access in this database. More internet access means a populations productivity also increases. People are able to access educational and self development resources at a low cost and some for free of charge. It is generally known that education improves quality of life, societies and economies benefit from individuals with a positive outlook on life.

Wireless communication is what makes technologies such as robotics, IoT and self driving cars possible. Wireless communication with robotics make it possible people to perform physical task remotely. Technological advances in health care are looking into remove surgical operations as a means of increasing health care reach. Wearables such as smart watches are also a technology which can be used to track your health more accurately and can be used to give more detailed medical records. Responsive equipment can be made that will be operated remote. That equipment will perform a certain function depending on the state of the client.

Business also benefit from Wifi. Wifi availability is usually at the top of peoples list when visiting a place such a a mall or restaurant. This is because WiFi a source of enjoyment from the otherwise uneventful trip to a mall and people tend to spend more time in restaurant with WiFi which means they are also more likely to spend more. WiFi is also used a source of entertainment, you can stream, download content from the Internet. The biggest benefactors of wireless networks are rural communities and schools. WiFi allows people in rural areas to access information which would be challenge otherwise

because of the to huge distance one would have to travel. The internet can be used as an alternative source of information complementary to ones school resources.

3 Challenges and Solution

As more people use the internet the more challenging it becomes for communication systems to cope with the increasing internet demands. Network congestion and drop happens more frequently to saturated networks. This problem usually leaves many users frustrated and business may lose customer due to their services being unreliable as a result of not being able to connect in time with customers. Is it important to address this problem in order to avoid buffering videos, time out file downloads and freezing video calls. Network resources are limited by hardware and software advancements. It is therefore important to try to free up some of these network resources by providing more options to users. The proposed engineering solution is developed with aim of increasing the rate at which the end user can receive information. The presented solution is for WiFi router, which is a device owned by many. The solution is designed with sustainable and impact in mind.

The solution present is able to meet current traffic demands and has comparable specifications as some commercial product. However it falls short in being a viable solution for the future.

4 Conclusion

Wireless communication provides an easy and cheap way of accessing the internet. Wifi is powering some the latest technologies such as robotics, IoT and self driving cars. Business and individuals positively benefit from good internet coverage. Wireless infrastructure is under stress due to huge number of internet users. Infrastructure inefficiencies contributes to poor reception which might leave users with a negative experience. It is therefore important to improve the underlying infrastructure in order to improve the user experience.

APPENDIX B Course Objectives: ECSA ELOs

The ELO indicate the requirements the student is expected to meet in order to satisfy in order to pass the course. The outcomes mainly cover the following:

- A design that considers social, economic or environmental impact and is also sustainable.
- Must make use of engineering concepts.
- Complete the project with limited supervision.
- Documenting the project design and findings.

Table B.1: ECSA ELOs topic coverage

ELO	**Section in report**
3	Technical report
1	Technical report
2	section 4 and section 6
5	section 4 , subsection 2 .5 and section 6
7a	section 7
7b	section 8
8a	section 9
6a	Technical report
6b	Appendix A

The table shows the approximate time spent on each task. The table was developed at the beginning of the project along side the project plan.

Table B.2: Approximate time distribution

Task	**Time spent**
AMC research and early design	16%
Design implementation	18%
AMC regions	18%
Machine learning	18%
Documentation	30 %

APPENDIX C Design factors

The plot below is used to determine the 3 QAM modulating levels for the MCSs. Performances drops as the modulation order is increased. The performance comparison is done in AWGN but we expect similar result in Rayleigh.

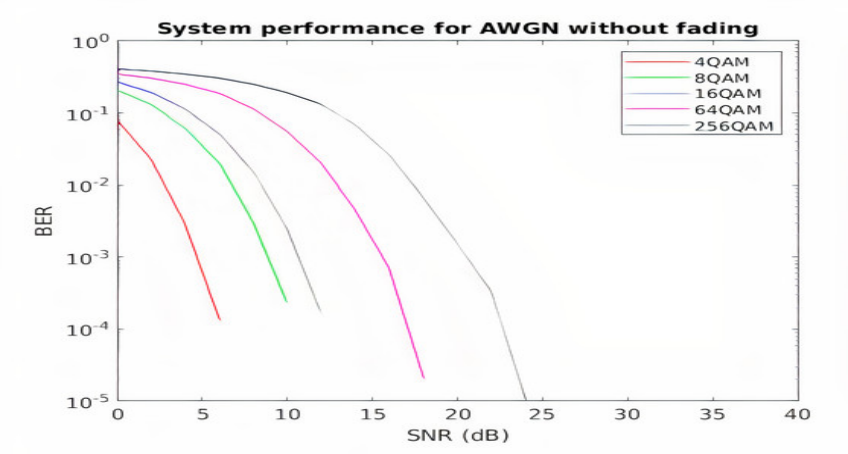

Fig. C.1: QAM SNR vs BER curves

The following figures show the constellations of the various in the channel. The constellation of a M-ary modulator can be calculated using the equation below.

$$s_m(t) = A_{c,m}cos(2\pi f_c t) + A_{q,m}sin(2\pi t) \tag{C.1}$$

$m = 1, 2, ...M$ and, $A_{c,m}$ and $A_{c,m}$ are integers from mapping a bit sequence into a signal.

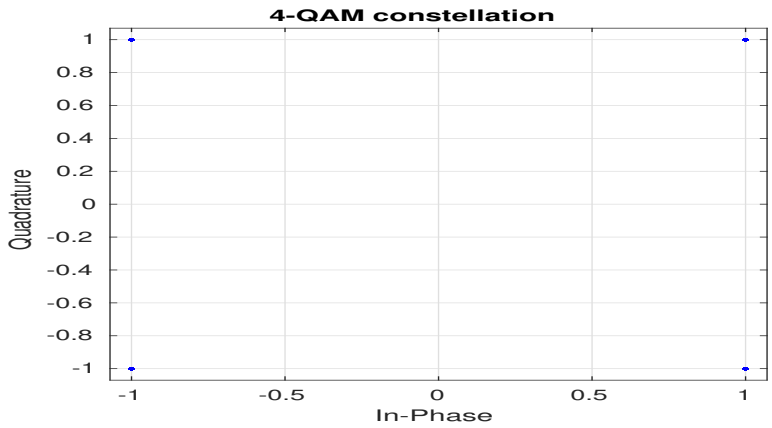

Fig. C.2: 4QAM constellation at SNR = 40

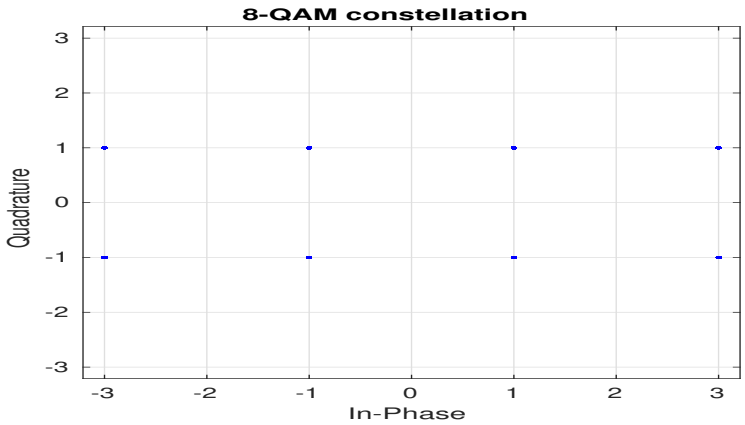

Fig. C.3: 8QAM constellation at SNR = 40

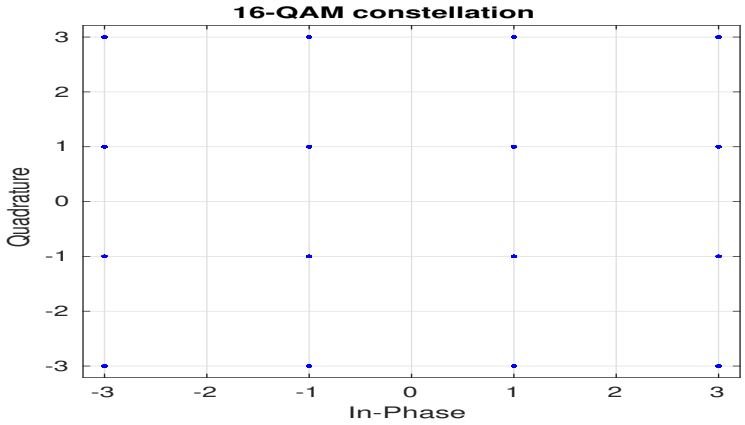

Fig. C.4: 16QAM constellation at SNR = 40

APPENDIX D Fading Characteristics

Below is the SNR vs BER curves for the chosen MCS at high correlation. We see that high correlation means the channel is close to AWGN like in Figure C.1 because the G_f has negligible effects.

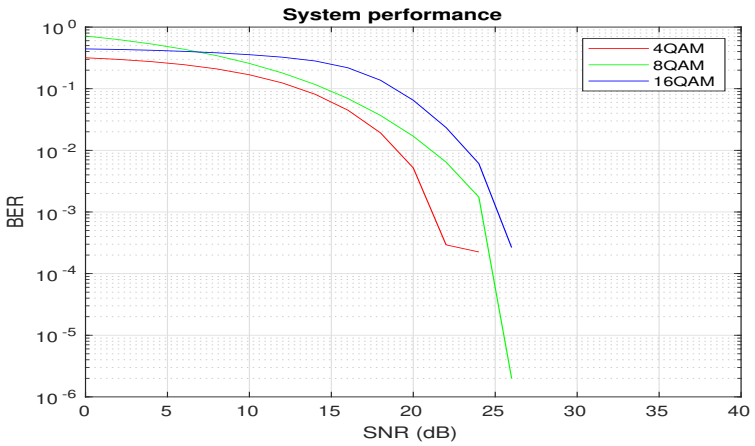

Fig. D.1: High correlation $\alpha = 0.99$ and $\sigma_g^2 = 3$, SNR vs BER.

The MCS experiences extreme fading when the channel has low correlation. We see that the curves are linear meaning they have a constant BER drop.

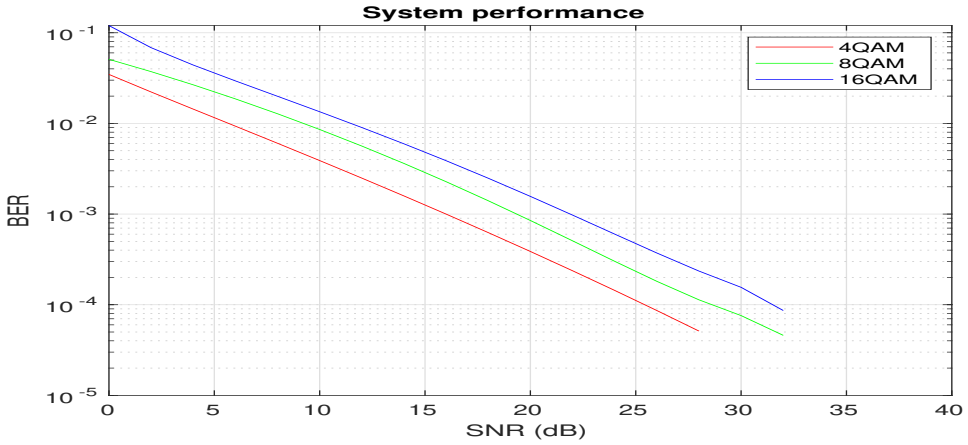

Fig. D.2: low correlation $\alpha = 0.1$ and $\sigma_g^2 = 3$, SNR vs BER.

Figure Figure D.3 is the corresponding ζ plot. The plot is not be perfectly linear due to $\mathbf{G}_f$ still being present. It is even more clear to observe the high correlation of the channel in this plot.

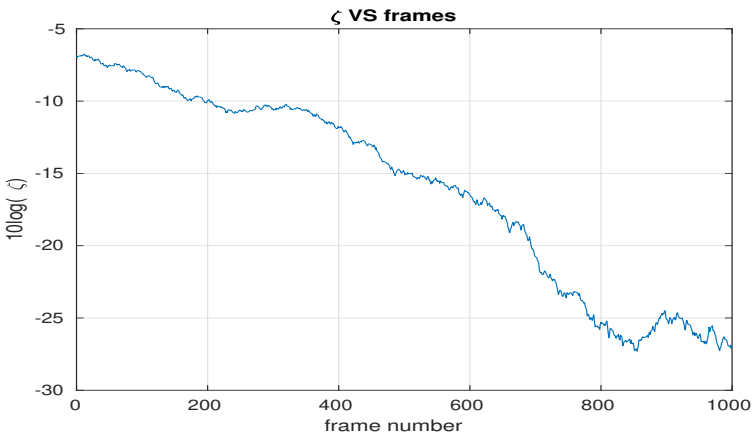

Fig. D.3: High correlation $\alpha = 0.99$ and $\sigma_g^2 = 3$, ζ plot.

In contrast this figure shows a high channel variation as a result of low channel correlation.

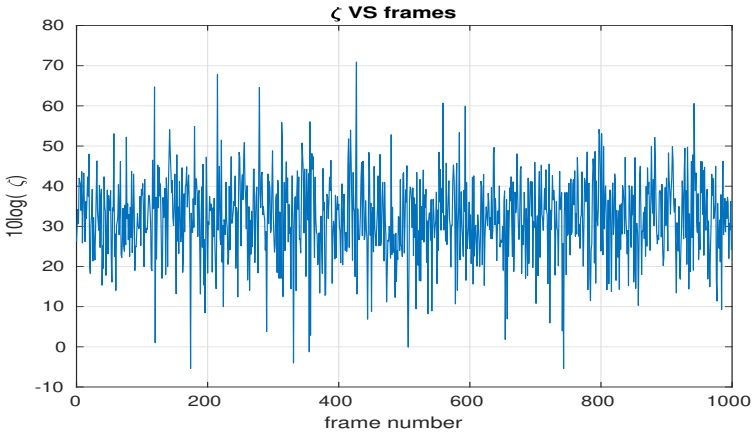

Fig. D.4: Low correlation $\alpha = 0.1$ and $\sigma_g^2 = 3$, ζ plot.

APPENDIX E Simulation Code Listing

```
%% AMC System simulation
% Date: 21 August 2020
% Autho: Sbonelo Mdluli
% Student Number: 1101772
%%
clear
clc
warning('off')

n = 15;
k = 5;
Tx = 2;              %  number of Tx antennas

fig = figure;
grid on;
ax = fig.CurrentAxes;
hold(ax,'on');


gf_square = 3 ;%0:1:10;
a = 0.96; %0:0.1:1;
frame_size = 2000;
no_frames = 1000;
SNR = 0:2:40;
figure

enc = comm.BCHEncoder(n,k);

dec = comm.BCHDecoder(n,k);


errorRate = comm.ErrorRate;
errorCalc2 = comm.ErrorRate;
errorCalc3 = comm.ErrorRate;

qam16_error = zeros(3,21);
qam8_error = zeros(3,21);
qam4_error = zeros(3,21);

prefectPred_error = zeros(3,21);


zeta16qam = zeros(1,no_frames);
states = zeros(1,no_frames);


% keep track of how many times a system is in use
sy1num =0;
sy2num =0;
sy3num =0;

for n= 1:length(a)

    for m = 1:length(gf_square)
```

```
55
56      for pos = 1:length(SNR)
57          reset(errorRate);
58          reset(errorCalc2);
59          reset(errorCalc3);
60          H = complex(eye(Tx,Tx))/sqrt(2); % normalised
61          for bits = 1:no_frames
62              H_herrm = ctranspose(H); % H^H matrix
63
64              data = randi([0 1], frame_size, 1); % generate random bits
65              encodedData = enc(data);
66
67              QAM16 = qammod(encodedData,16,'InputType','bit');
68              QAM8 = qammod(encodedData,8,'InputType','bit');
69              QAM_4 = qammod(data,4,'InputType','bit');
70
71              Es16 = mean(abs(QAM16).^2); % calculate energy
72              Es8 = mean(abs(QAM8).^2);
73              EsQAM4 = mean(abs(QAM_4).^2);
74
75              X = (reshape( QAM16, Tx, [])); % convert to serial parrallel stream, 16
                    QAM
76              xq = (reshape( QAM8, Tx, [])); % 8QAM
77              xpsk = (reshape( QAM_4, Tx, [])); % 4QAM
78
79
80              sigSquared = (Es16*n*10^(-SNR(pos)/10))/(k*log2(16));
81              sigSquared8qam = (Es8*n*10^(-SNR(pos)/10))/(k*log2(8));
82              sigSquared4QAM = (EsQAM4*n*10^(-SNR(pos)/10))/(k*log2(4));
83
84              sig = sqrt(sigSquared);
85              sig8qam = sqrt(sigSquared8qam);
86              sig4QAM = sqrt(sigSquared4QAM);
87
88              N16qam = (sig/sqrt(2))*(normrnd(0,1,[Tx,1]) + 1i*normrnd(0,1,[Tx,1])); %
                     noise matrix
89              N8qam = (sig8qam/sqrt(2))*(normrnd(0,1,[Tx,1]) + 1i*normrnd(0,1,[Tx,1]))
                    ; % noise matrix
90              N4qam = (sig4QAM/sqrt(2))*(normrnd(0,1,[Tx,1]) + 1i*normrnd(0,1,[Tx,1]))
                    ; % noise matrix
91
92              W16QAM = ((H_herrm*H+sigSquared*eye(Tx,Tx))^-1)*(H_herrm);
93              W8qam = ((H_herrm*H+sigSquared8qam*eye(Tx,Tx))^-1)*(H_herrm);
94              W4QAM = ((H_herrm*H+sigSquared4QAM*eye(Tx,Tx))^-1)*(H_herrm);
95
96              Y_hat = W16QAM*(H*X +N16qam);%16QAM
97              Yhatqam = W8qam*(H*xq +N8qam);%8QAM
98              Y_hatPsk = W4QAM*(H*xpsk +N4qam); % 8PSK
99
100             outRx16 = Y_hat(:); % 16QAM
101             outRx8 = Yhatqam(:);% 8QAM
102             outRx4 = Y_hatPsk(:);% 8QAM
103
104
105             demodSignal = qamdemod(outRx16,16,'OutputType','bit'); % 16QAM
106             qamdemodout = qamdemod(outRx8,8,'OutputType','bit'); % 8QAM
```

```
            pskmodout = qamdemod(outRx4,4,'OutputType','bit');

            received16QAM = dec(demodSignal);
            received8QAM = dec(qamdemodout);


            qam4_error(:,pos) = errorCalc3(data, pskmodout); % 4QAM
            qam16_error(:,pos) = errorRate(data, received16QAM); % 16QAM
            qam8_error(:,pos) = errorCalc2(data, received8QAM); % 8QAM

            GF = normrnd(0,gf_square(m),Tx,Tx) + 1i*normrnd(0,gf_square(m),Tx,Tx);
            H = a(n)*H+(1-a(n))*GF; %;


            if SNR(pos) == 30 %assuming perfect channel prediction
                zeta16qam(1,bits) = 10*log(abs(sum((H*W16QAM).^2,'all')/sum(W16QAM
                    .^2,'all')));

                if zeta16qam(1,bits) < -15
                    states(:,bits) = 1;
                    sy1num = sy1num +1;
                    prefectPred_error (:,pos) = errorCalc3(data, pskmodout);
                elseif zeta16qam(1,bits) > -5
                    states(:,bits) = 3;
                    sy3num = sy3num +1;
                    prefectPred_error (:,pos) = errorCalc3(data, pskmodout);
                else
                    states(:,bits) = 2;
                    sy2num = sy2num +1;
                    prefectPred_error (:,pos) = errorRate(data, received16QAM);
                end
            end


            zeta16qam(1,bits) = 10*log(abs(sum((H*W16QAM).^2,'all')/sum(W16QAM.^2,'
                all')));

            if zeta16qam(1,bits) < -15

                prefectPred_error (:,pos) = errorCalc3(data, pskmodout);
            elseif zeta16qam(1,bits) > 0

                prefectPred_error (:,pos) = errorCalc3(data, pskmodout);
            else

                prefectPred_error (:,pos) = errorRate(data, received16QAM);
            end



        end

    end

    %BER curve fitting
    QAM16 = berfit(SNR, qam16_error(1,:));
```

```
161     QAM8 = berfit(SNR, qam8_error(1,:));
162     QAM4 = berfit(SNR, qam4_error(1,:));
163     perfect = berfit(SNR, prefectPred_error(1,:));
164
165     tiledlayout(4,1)
166
167     SNR1 = SNR(:,1:length(QAM4));
168     SNR2 = SNR(:,1:length(QAM8));
169     SNR3 = SNR(:,1:length(QAM16));
170     SNR4 = SNR(:,1:length(perfect));
171
172
173     semilogy(SNR1,  QAM4, 'r', ...
174         SNR2, QAM8, 'g',...
175         SNR3, QAM16, 'b',...
176         SNR4, perfect, 'm')
177
178     legend('4QAM',...
179         '8QAM', ...
180         '16QAM',...
181         'PERFECT PRed');
182     xlabel('SNR (dB)');
183     ylabel('BER');
184
185     title('System performance');
186     xlim([SNR(1), SNR(end)]);
187
188     nexttile
189
190     x = 0:1:no_frames-1;
191     plot(x, zeta16qam);
192     title('\zeta VS frames');
193     ylabel('10log(\zeta)') ;
194     xlabel('frame number') ;
195
196     avg = mean(zeta16qam);
197
198
199     dataRate = (10^-3)*(sy1num*log2(4) + sy2num*log2(8)*(1/3) + sy3num*log2(16)
            *(1/3))*(2);
200     % 2 antenna
201     % 1/3 encoder
202     % threshold is 10^-3
203      %a(n)
204    % scatter3(a(n),gf_square(m),dataRate,'*')
205    % view(-30,10)
206    % xlabel('\alpha')
207    % ylabel('\sigma')
208    % zlabel('Data rate')
209
210
211     % title('Data rate as a function of \alpha and \sigma')
212     % hold on;
213
214      %   drawnow;
215
```

```
    end

end

data = vertcat(zeta16qam,states);
writematrix(data)
writematrix(states)
```

```
%% LSTM AMC simulation
% Date: 21 August 2020
% Autho: Sbonelo Mdluli
% Student Number: 1101772
%%
data = readmatrix('data.txt');

numTimeStepsTrain = floor(0.9*numel(data));

dataTrain = data(1:numTimeStepsTrain+1);
dataTest = data(numTimeStepsTrain+1:end);

no_frames = 1000;

LSTMstates = zeros(1,no_frames);

mu = mean(dataTrain);
sig = std(dataTrain);

dataTrainStandardized = (dataTrain - mu) / sig;

XTrain = dataTrainStandardized(1:end-1);
YTrain = dataTrainStandardized(2:end);

numFeatures = 1;
numResponses = 1;
numHiddenUnits = 250;

layers = [ ...
    sequenceInputLayer(numFeatures)
    lstmLayer(numHiddenUnits)
    fullyConnectedLayer(numResponses)
    fullyConnectedLayer(numResponses)
    regressionLayer];

options = trainingOptions('adam', ...
    'MaxEpochs',250, ...
    'GradientThreshold',1, ...
    'InitialLearnRate',0.005, ...
    'LearnRateSchedule','piecewise', ...
    'LearnRateDropPeriod',110, ...
    'LearnRateDropFactor',0.09, ...
    'Verbose',0, ...
    'Plots','training-progress');

net = trainNetwork(XTrain,YTrain,layers,options);
```

```
48
49 mu = mean(dataTrain);
50 sig = std(dataTrain);
51
52 dataTestStandardized = (dataTest - mu) / sig;
53 XTest = dataTestStandardized(1:end-1);
54 YTest = dataTest(2:end);
55 YPred = [];
56 numTimeStepsTest = numel(XTest);
57 for i = 1:numTimeStepsTest
58     [net,YPred(:,i)] = predictAndUpdateState(net,XTest(:,i),'ExecutionEnvironment','
        cpu');
59 end
60
61 % keep track of how many times a system is in use
62 sy1num =0;
63 sy2num =0;
64 sy3num =0;
65
66 YPred = sig*YPred + mu;
67
68 rmse = sqrt(mean((YPred-YTest).^2))
69 pos =1;
70
71
72 for i = 1:numTimeStepsTest
73             if YPred(1,i) < -15
74
75                 LSTMstates (:,pos) = 1;
76                 pos = pos+1;
77                 sy1num = sy1num +1;
78             elseif YPred(1,i) > 0
79
80                 LSTMstates (:,pos) = 3;
81                 pos = pos+1;
82                 sy3num = sy3num +1;
83             else
84
85                 LSTMstates (:,pos) = 2;
86                 pos = pos+1;
87                 sy2num = sy2num +1;
88             end
89 end
90
91
92 dataRate2 = (10^-3)*(sy1num*log2(4) + sy2num*log2(8)*(1/3) + sy3num*log2(16)*(1/3))
    *(2);
93
94 figure
95 subplot(2,1,1)
96 plot(YTest)
97 hold on
98 plot(YPred,'.-')
99 hold off
100 legend(["Observed" "Predicted"])
101 ylabel("zeta")
```

```
xlabel("frames")
title("LSTM zeta predictor")

writematrix(LSTMstates)
```

```
%% NN AMC simulation
% Date: 21 August 2020
% Autho: Sbonelo Mdluli
% Student Number: 1101772
%%
data = readmatrix('data.txt');

frame = 0:1000;

y = num2cell(data(1:900));

ftdnn_net = timedelaynet([1:4],10);
ftdnn_net.trainParam.epochs = 1000;
ftdnn_net.divideFcn = '';

p = y(5:end);
t = y(5:end);
Pi=y(1:4);
ftdnn_net = train(ftdnn_net,p,t,Pi);

yp = ftdnn_net(p,Pi);
e = gsubtract(yp,t);
rmse = sqrt(mse(e))

% keep track of how many times a system is in use
sy1num =0;
sy2num =0;
sy3num =0;


pos =1;
frameSize = 1000;


yp = cell2mat(yp);
NNstates = zeros(1,length(yp));

for i = 1:length(yp)
            if yp(1,i) < -15

                NNstates (:,pos) = 1;
                pos = pos+1;
                sy1num = sy1num +1;
            elseif yp(1,i) > 0

                NNstates (:,pos) = 3;
                pos = pos+1;
                sy3num = sy3num +1;
            else

                NNstates (:,pos) = 2;
```

```
52                  pos = pos+1;
53                  sy2num = sy2num +1;
54              end
55  end
56
57  dataRate1 = (10^-3)*(sy1num*log2(4) + sy2num*log2(8)*(1/3) + sy3num*log2(16)*(1/3))
        *(2);
58
59  writematrix(NNstates)
```

APPENDIX F Project Planning

Fig. F.1: Project plan timeline

APPENDIX G Engineering Notebook

28/04/2020

ELEN 4011 (INF DESIGN)

5 weeks

- code rate ⇒ 2 bits/Hz
- Channel bandwidth of 4 MHz
- Employ MIMO to combat fading
- data rate of 10 M bits/s

⇒ Make simulation using MATLAB

- {Random bits}

⇒ System design

- ∞ fixed Antenna
- Vary Tx & Rx

min freedom
↓ syst

⇒ Make the simulation (due next monday)

↙ Matlab2020 (email)

Avail
[Wed - Friday]

27/07/2020 →

RCH codes vs Reed Solomon

- matrix size dependent on number of Antennas
- Q_m (transmitter π)

for each SNR

$$P_n = \frac{\pi \cdot N \text{ error}}{\text{transmitted bits}}$$

fec → encoder → modulator → mimo

Send → parallel

W → equalizer

what is H??

N = Normalized

Avoid padding

Of per frame

pulse shaping (No)

weak filter

03/08/2020

MIMO Spectral efficiency

* Sacrifice performance

N-2 Antennas

R=3
M=2
$d_m = 2$

$\frac{1}{3}(2 \times 1) = 0,66 \Rightarrow$ don't need specs

[8 PSK
8 QAM
16 PSK] → get curves for systems

- F - frame (1000 frames / min)

$\sigma_s = (0,1 - 0,5)$
2/4 encoder

* Must make serial to parallel
- BER not dipping early (straight line)

$$\zeta = \frac{\Sigma\Sigma z}{\Sigma\Sigma w}$$

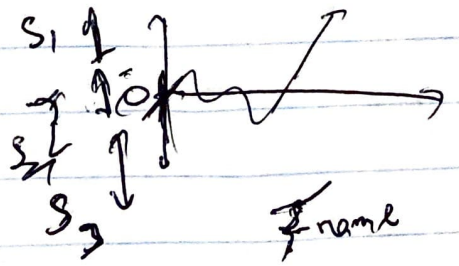

BCH $(N = 15, K = 5)$ $\sim \frac{1}{3}$ encoder

$\frac{1}{3}(3)(2) = 3 \Rightarrow 2$

$\Rightarrow$ Currently testing using AWGN

$\Rightarrow$ Model not working

SNR curve ~~not~~ Gradient not falling

Try

change FEC

MIMO

BER $\sim 10^{-1}$

$SNR = 10 \log_{10}\left(\frac{E_s}{N_0}\right)$

$10^{-\frac{SNR}{10}}$

$H_f = \alpha(H_{f-1} - G_t) + G_f$

Set $H = I$ (initial) . (testing)

10/08/2020

* MMSE detector over ZF

$\sigma^2 >> 0$

Post detection {SNR}

$\lambda = \sigma^2 = \frac{N_0}{2}$

$E[xx^H] = \frac{P}{nt} I$

$\sigma = \frac{1}{\sqrt{2}} (\sqrt{N_0})$ → constellation

Energy per symbol

$(N*N)(N*1) + (N*1) = N*1$

Radio waves

→ MIMO capacity G

Auto correlation function

22/ 2/20

- Briefly W^2
- what happens if BER not meet
  ↓
  retransmit or ack

→ α → role
→ How we got to the channel model C_f??